ACS OMEGA

Article

http://pubs.acs.org/journal/acsodf

Structure–Property Relationships of Poly(ethylene carbonate) and Poly(propylene carbonate)

Yuji Sasanuma* and Yuta Takahashi

Department of Applied Chemistry and Biotechnology, Graduate School and Faculty of Engineering, Chiba University, 1-33 Yayoi-cho, Inage-ku, Chiba 263-8522, Japan

Supporting Information

ABSTRACT: Conformational characteristics of poly(ethylene carbonate) (PEC) and poly(propylene carbonate) (PPC) have been revealed via molecular orbital (MO) calculations and nuclear magnetic resonance (NMR) experiments on model compounds with the same bond sequences as those of the polycarbonates. Bond conformations derived from the MO calculations on the models were in exact agreement with those from the NMR experiments. Both PEC and PPC were indicated to adopt distorted conformations including a number of gauche bonds and cover themselves with negative charges, thus failing to form a regular packing and remaining amorphous. The MO data were applied to the refined rotational isomeric state (RIS) calculations to yield configurational properties such as the characteristic ratio, its temperature coefficient, the configurational entropy, and average geometrical parameters of unperturbed PEC and PPC chains. In the RIS calculations on PPC, the regio- and stereosequences were generated according to the Bernoulli trial or Markov stochastic process. In consequence, it was shown that the configurational properties of PPC do not depend significantly on its regio- and stereoregularities. The internal energy contribution to rubberlike chain elasticity, calculated from the temperature coefficient of the characteristic ratio, has indicated the possibility that PEC and PPC will behave as elastomers. The practical applications and potential utilizations of the polycarbonates are discussed on the basis of the conformational characteristics and configurational properties.

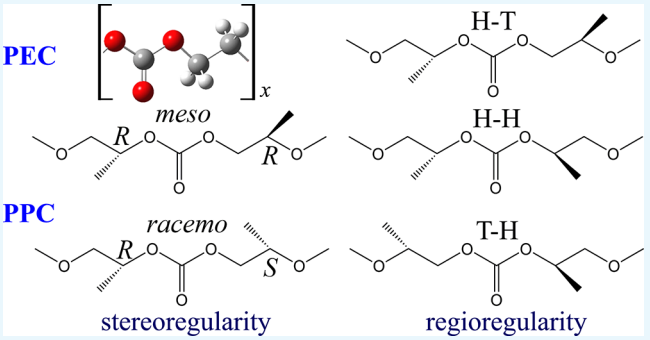

INTRODUCTION

If noxious fumes generated in industrial processes were dispersed into the atmosphere, animals including human beings and plants would be seriously injured or, at their worst, killed. However, chemists have settled such problems by fixing the gases in solids. For example, in alkali industries, gaseous chlorine generated in sodium production has been chemically changed to useful polymers such as poly(vinyl chloride).[1] As another example, one may mention carbon dioxide. Of course, carbon dioxide itself is not necessarily a harmful substance but, on the contrary, a nutrient source indispensable for plants. To suppress the global warming, however, we have been strongly required to control the amount of atmospheric carbon dioxide.

In 1969, Inoue, Koinuma, and Tsuruta[2,3] reported a reaction scheme to synthesize poly(alkyl carbonate)s, that is, alternating copolymers of epoxides with carbon dioxide (Scheme 1). In the reaction, carbon dioxide, the most inactive (i.e., thermodynamically dead) carbon source, is utilized. Because of the growing worldwide interest in global warming, polymer chemists and engineers have been paying particular attention to polycarbonates. If carbon dioxide emitted from combustion of natural gas, petroleum, and coal can be effectively absorbed on basic polymers such as poly(ethylene imine)[4−6] and its derivatives[7] and analogues,[8] the polycarbonates may be produced from the collected gas, and consequently, CO_2 fixation will be realized.

Scheme 1. Synthesis of Aliphatic Polycarbonates from Epoxides and Carbon Dioxide: R = H, Poly(ethylene carbonate) (PEC) and R = CH_3, Poly(propylene carbonate) (PPC)

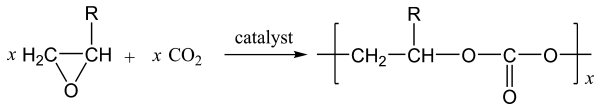

Of the aliphatic polycarbonates, PEC (Figure 1) and PPC were synthesized early[2,3] but have not been easy to use either as hard plastics or as flexible rubbers because glass transitions of PEC and PPC occur around room temperature (ca. 20 °C) and human body temperature (35−40 °C), respectively.[9] Therefore, the polycarbonates will become hard in cold areas (or seasons) but flexible in hot ones.

Inasmuch as PPC has an asymmetric carbon atom in the repeating unit, its primary structure is determined by two kinds

Received: July 21, 2017
Accepted: July 26, 2017
Published: August 22, 2017

DOI: 10.1021/acsomega.7b00964
ACS Omega 2017, 2, 4808−4819

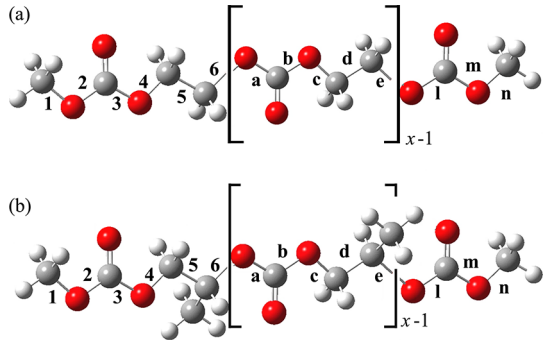

Figure 1. (a) PEC and (b) PPC. The bonds are designated as shown, and x is the degree of polymerization. To facilitate the refined rotational isomeric state (RIS) calculations, the polymeric chains have been assumed to be terminated by a methyl group.

of configurations: stereo- and regioisomerizations. The former means the existence of (*R*)- and (*S*)-isomers (see Figure 2). The latter means the formation of three kinds of linkages between the monomeric units: head-to-tail (abbreviated as H−T), head-to-head (H−H), and tail-to-tail (T−T) (see Figure 3). For these reasons, polymer chemists have challenged to develop stereospecific catalysts for controlling its regio- and stereoregularities,[10−22] in expectation that fully regular PPCs

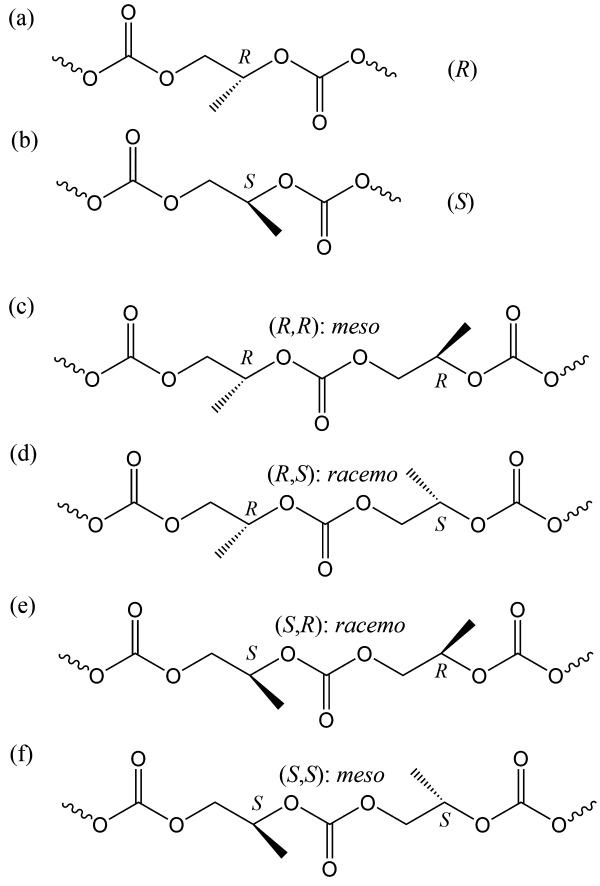

Figure 2. Stereosequences of PPC: (a) (*R*)- and (b) (*S*)-isomers; (c) (*R*,*R*)-, (d) (*R*,*S*)-, (e) (*S*,*R*)-, and (f) (*S*,*S*)-diads. (*R*,*R*)- and (*S*,*S*)-diad combinations are designated as *meso*, and (*R*,*S*)- and (*S*,*R*)-diad ones as *racemo*. When the polymeric chain is composed of only *meso* (*racemo*) couplings, the stereoregularity is termed isotactic (syndiotactic).

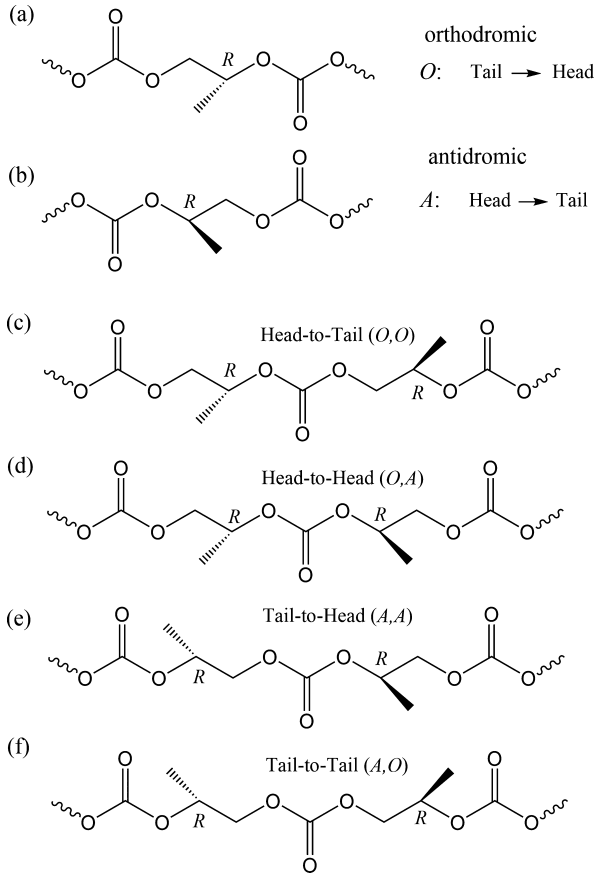

Figure 3. Regiosequences of PPC. Definition of (a) orthodromic (*O*) and (b) antidromic (*A*) directions. Four possible combinations of (*O*)- and (*A*)-directions between neighboring units: (c) (*O*,*O*), head-to-tail (H−T); (d) (*O*,*A*), head-to-head (H−H); (e) (*A*,*A*), tail-to-head (T−H); and (f) (*A*,*O*), tail-to-tail (T−T). The tail-to-head linkage is included in H−T; therefore, the three expressions, H−T, H−H, and T−T, are used herein.

might crystallize and exhibit so large an elastic modulus and so high a glass transition temperature (T_g) as to be used as hard plastics.

According to a cardinal principle of polymer science and molecular biology, "higher-order structures, physical properties, and functions of a polymer originate from its primary structure"; it is of fundamental importance to reveal the conformational characteristics of PEC and PPC and, furthermore, to evaluate their configurational properties. This is the prime aim of this study. The conformational analysis of model compounds with the same bond sequences as those of the polycarbonates, ethylene glycol bis(methyl carbonate) (E_model, Figure 4) for PEC and propylene glycol bis(methyl carbonate) (P_model) for PPC, has been carried out by molecular orbital (MO) calculations and nuclear magnetic resonance (NMR) experiments. The MO energies and geometrical parameters were introduced into the refined RIS scheme[23] to yield configurational properties of the two polycarbonates. Then, stochastic processes based on the Bernoulli trial and first-order Markov chain[24,25] were employed to generate regio- and stereosequences of PPC to elucidate how its properties depend on the two kinds of configurations. Herein, the procedures and results are described in detail. On the basis of the structural information thus established, physical

DOI: 10.1021/acsomega.7b00964
ACS Omega 2017, 2, 4808−4819

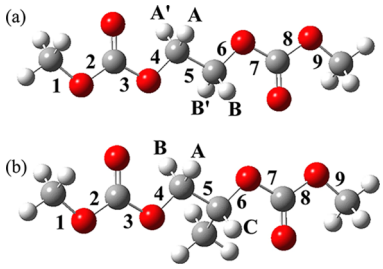

Figure 4. Model compounds of PEC and PPC: (a) for PEC, ethane-1,2-diyl dimethyl bis(carbonate) (E_model) and (b) for PPC, dimethyl propane-1,2-diyl bis(carbonate) (P_model). As indicated, the bonds are designated, and the methylene and methine protons are labeled for NMR analysis. (*R*)- and (*S*)-P_models yield the identical NMR spectra; therefore, (*R*)-P_model is exclusively employed herein.

properties, practical uses, and potential applications of PEC and PPC are discussed.

RESULTS AND DISCUSSION

NMR Experiments. Figure 5a shows ^{1}H NMR satellite peaks observed from the naturally abundant $^{13}CH_2$ group of the

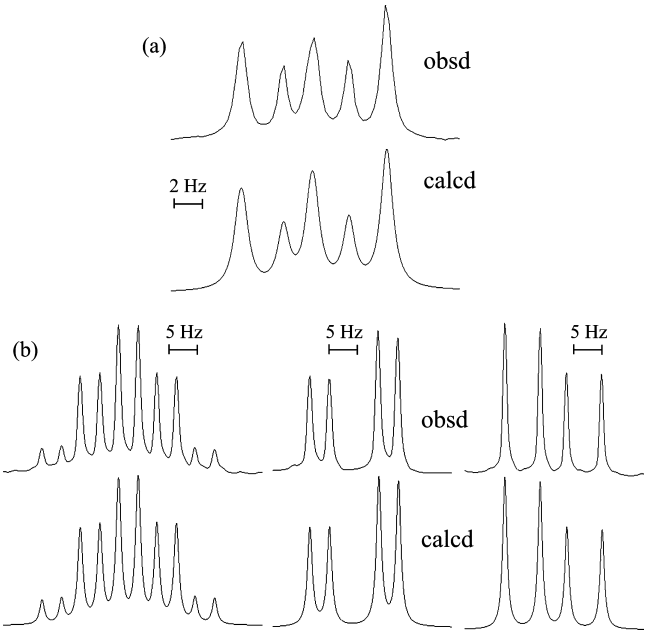

Figure 5. Observed (above) and calculated (below) ^{1}H NMR spectra: (a) satellite from the CH_2 group of the E_model dissolved in dimethyl-d_6 sulfoxide (DMSO-d_6) at 25 °C; (b) H_C (left), H_A (middle), and H_B (right) of the P_model dissolved in $CDCl_3$ at 25 °C. For the proton symbols of the P_model, see Figure 4.

E_model. The spectrum simulation reproduced the observation well and yielded the J_{HH} and J'_{HH} values. In Table 1, the two vicinal couplings are given for each NMR solvent and temperature. As explained in the "Methods" section, the p_t and p_g values were derived from eqs 8 and 9 with the two sets of J_T and J_G. The sum of p_t and p_g, thus obtained was slightly different from unity and hence divided by the sum to fulfill eq 10. The p_t values of bond 5 (Table 2) are so small as to indicate a strong gauche preference of the CH_2−CH_2 bond, and the p_t value tends to increase with temperature and decrease slightly with solvent polarity.

Table 1. Observed NMR Vicinal ^{1}H−^{1}H Coupling Constants of E_Model[a]

solvent	permittivity	temp (°C)	J_{HH}	J'_{HH}
chloroform-*d*	4.8	15	6.46	2.70
		25	6.46	2.81
		35	6.46	2.89
		45	6.45	2.97
		55	6.44	3.05
acetone-d_6	20.7	15	6.52	2.60
		25	6.49	2.65
		35	6.49	2.70
		45	6.48	2.76
methanol-d_4	32.7	15	6.48	2.58
		25	6.47	2.61
		35	6.46	2.67
		45	6.46	2.75
		55	6.46	2.82
DMSO-d_6	46.7	25	6.49	2.48
		35	6.49	2.53
		45	6.48	2.60
		55	6.47	2.69

[a]In Hz.

Table 2. Trans Fractions (p_t's) of E_Model: Comparison between MO Calculations and NMR Experiments

		bond 4 (6)	bond 5		
				NMR	
medium	temp (°C)	MO	MO	set A	set B
gas	15	0.39	0.12		
	25	0.39	0.12		
	35	0.39	0.13		
	45	0.39	0.13		
	55	0.38	0.14		
chloroform	15	0.51	0.06	0.01	0.05
	25	0.50	0.07	0.02	0.06
	35	0.50	0.07	0.03	0.07
	45	0.49	0.07	0.04	0.08
	55	0.49	0.08	0.04	0.08
acetone	15	0.55	0.04	0.00	0.04
	25	0.54	0.05	0.01	0.05
	35	0.53	0.05	0.02	0.05
	45	0.53	0.05	0.02	0.06
methanol	15	0.55	0.04	0.00	0.04
	25	0.55	0.04	0.01	0.04
	35	0.54	0.05	0.01	0.05
	45	0.53	0.05	0.02	0.06
	55	0.53	0.06	0.03	0.06
DMSO	25	0.55	0.04	~0.00	0.03
	35	0.54	0.05	~0.00	0.03
	45	0.54	0.05	0.01	0.04
	55	0.53	0.06	0.01	0.05

In Figure 5b, ^{1}H NMR spectra observed from H_A, H_B, and H_C of the P_model are shown, together with the spectrum simulations. The obtained J_{AB} and J_{BC} values (Table 3) were substituted into eqs 11 and 12 to yield the bond conformations as shown in Table 4. The magnitude relation of $p_t \ll p_{g^-} < p_{g^+}$ always holds regardless of the solvent and temperature.

MO Calculations. Table 5 shows conformer free energies of the E_model. Of the eight conformers that the B3LYP optimization gave, the most stable conformation is tg$^+$t (Figure

DOI: 10.1021/acsomega.7b00964
ACS Omega 2017, 2, 4808−4819

Table 3. Observed NMR Vicinal $^1H-^1H$ Coupling Constants of P_Model[a]

solvent	temp (°C)	J_{AC}	J_{BC}
chloroform-*d*	15	6.85	3.32
	25	6.80	3.34
	35	6.71	3.43
	45	6.60	3.51
	55	6.58	3.55
acetone-d_6	15	6.82	3.06
	25	6.75	3.11
	35	6.68	3.16
	45	6.66	3.20
methanol-d_4	15	6.80	3.10
	25	6.77	3.15
	35	6.75	3.21
	45	6.70	3.25
	55	6.65	3.31
DMSO-d_6	25	6.76	2.93
	35	6.70	2.96
	45	6.66	3.00
	55	6.60	3.04

[a]In Hz.

Table 4. Bond Conformations of (*R*)-P_Model Determined from NMR Experiments

		bond 5					
		set A			set B		
solvent	temp (°C)	p_t	p_{g^+}	p_{g^-}	p_t	p_{g^+}	p_{g^-}
chloroform	15	0.10	0.59	0.31	0.11	0.50	0.39
	25	0.11	0.58	0.31	0.11	0.50	0.39
	35	0.12	0.57	0.31	0.12	0.49	0.39
	45	0.13	0.56	0.31	0.13	0.48	0.39
	55	0.14	0.55	0.31	0.14	0.47	0.39
acetone	15	0.07	0.56	0.37	0.08	0.50	0.42
	25	0.08	0.55	0.37	0.09	0.49	0.42
	35	0.08	0.54	0.38	0.10	0.48	0.42
	45	0.09	0.53	0.38	0.10	0.48	0.42
methanol	15	0.08	0.55	0.37	0.09	0.49	0.42
	25	0.08	0.55	0.37	0.09	0.49	0.42
	35	0.09	0.55	0.36	0.10	0.49	0.41
	45	0.10	0.54	0.36	0.11	0.48	0.41
	55	0.10	0.54	0.36	0.11	0.48	0.41
DMSO	25	0.05	0.55	0.40	0.07	0.49	0.44
	35	0.06	0.54	0.40	0.07	0.49	0.44
	45	0.06	0.54	0.40	0.08	0.48	0.44
	55	0.07	0.53	0.40	0.08	0.47	0.45

6a), indicating a gauche preference of the central CH_2-CH_2 bond. It has been found that the aromatic and aliphatic esters with the $C(=O)-O-CH_2-CH_2-O-C(=O)$ bond sequence show strong gauche preferences in the central CH_2-CH_2 bond. The free energies of the tgt conformation were evaluated as, for example, −1.1 kcal mol^{-1} for poly(ethylene terephthalate) (PET)[26] and −1.2 kcal mol^{-1} for poly(ethylene succinate) (PES).[27] These ΔG_k values are comparable to that of PEC (Table 5). Therefore, it can be concluded that the tgt stability is inherent in the $C(=O)-O-CH_2-CH_2-O-C(=O)$ sequence of the esters. The ttg$^+$ conformer also has a small free energy of 0.1−0.3 kcal mol^{-1} as compared with that of poly(ethylene oxide) (PEO) (1.3 kcal mol^{-1}).[28−30] It is also known that the ttg conformations of PET and PES have relatively small ΔG_k values of 0.5 and 0.3 kcal mol^{-1}, respectively.[26,27] In the ttg$^+$ conformation (Figure 6b), a short C═O···C−H contact (2.40 Å) can be found between the carbonyl and methylene groups via the gauche $O-CH_2$ bond, and the involved $O{=}C-O-CH_2-C-H$ atoms lie on a plane. The above results indicate that the PEC chain tends to adopt distorted structures with a number of gauche bonds. In Table 2, the bond conformations calculated from the ΔG_k values are listed. As for the CH_2-CH_2 bond, the MO calculations agree satisfactorily with set A and exactly with set B. These facts show the reliability of the MO energies.

Table 6 shows the ΔG_k values of P_model. Its asymmetric carbon renders the 27 (=3^3) conformers unique and irreducible, and the pendent methyl group gives rise to intramolecular steric repulsions; however, P_model exhibits the conformational preferences and intramolecular interactions similar to those found for the E_model. A number of conformers have negative ΔG_k's. In particular, those of g^+g^+t and tg^+t and $g^+g^-g^-$ are largely negative; therefore, PPC will also adopt distorted structures. The bond conformations of P_model, calculated from the ΔG_k values, are listed in Table 7. For the $CH_2-CH(CH_3)$ bond, the magnitude relation $p_t \ll p_{g^-} < p_{g^+}$ holds, thus being consistent with the NMR analysis. On the basis of the good agreement between theory and experiment, we advanced to the refined RIS calculations on PEC and PPC with the ΔG_k energies and geometrical parameters (Tables S1 and S2, Supporting Information) of the models.

Refined RIS Calculations. The characteristic ratios ($\langle r^2\rangle_0/nl^2$), its temperature coefficients ($d\ln\langle r^2\rangle_0/dT$), configurational entropies (S_{conf}), and averaged geometrical parameters of unperturbed PEC and PPC chains at 25 °C are presented in Table 8. The PPC chain was assumed to be isotactic and include only the H−T linkage. The temperature coefficient at T_0 was calculated by the finite-difference method

$$\frac{d\ln\langle r^2\rangle_0}{dT}(T_0) \approx \frac{\ln[\langle r^2\rangle_0(T_0+\Delta T)/\langle r^2\rangle_0(T_0-\Delta T)]}{2\Delta T} \quad (1)$$

where T_0 and ΔT were set equal to 298.15 K (25 °C) and 1.00 K, respectively.

The $\langle r^2\rangle_0/nl^2$ values are 2.42−2.54 (PEC) and 2.26−2.36 (PPC), much smaller than those of PEO (5.2 at 34.5 °C),[29,32,33] PPO (6.0 at 50 °C),[31,34] and polyethylene (6.4−8.3 around 140 °C).[35−39] This is because both PEC and PPC have strong preferences for gauche conformations. The $d\ln\langle r^2\rangle_0/dT$ values of PEC and PPC show solvent dependence; the values decrease with increasing solvent polarity. The temperature coefficient of PEC changes its sign between gas and chloroform, whereas that of PPC always stays positive. These results will be discussed in the "Mechanical Properties" section.

The configurational entropy (often termed conformational entropy) can be calculated from

$$S_{conf} = \frac{R}{x}\left[\ln Z + T\frac{d(\ln Z)}{dT}\right] \quad (2)$$

where R is the gas constant, x is the degree of polymerization, T is the absolute temperature, and Z is the partition function of the whole chain. At a phase transition such as melting, the S_{conf} value corresponds to the entropy change at constant volume

DOI: 10.1021/acsomega.7b00964
ACS Omega 2017, 2, 4808−4819

Table 5. Conformer Free Energies (ΔG_k's) of Model Compounds of PEC and PEO, Evaluated by Ab Initio MO Calculations[a]

				PEC[b]					PEO[c]
k	conformation[d]			gas	chloroform	acetone	methanol	DMSO	gas
1	t	t	t	0.00	0.00	0.00	0.00	0.00	0.00
2	t	t	g^+	0.11	0.23	0.28	0.29	0.29	1.31
3	t	g^+	t	−0.81	−1.35	−1.59	−1.62	−1.64	0.19 (−0.08[e])
4	t	g^+	g^+	−0.59	−1.00	−1.20	−1.23	−1.25	1.28
5	t	g^+	g^-			(absent)[f]			0.26
6	g^+	t	g^+	1.90	1.89	1.85	1.84	1.84	2.74
7	g^+	t	g^-	0.59	0.82	0.87	0.88	0.88	2.61
8	g^+	g^+	g^+	−0.42	−0.45	−0.48	−0.49	−0.49	2.27
9	g^+	g^+	g^-	−0.72	−0.81	−0.89	−0.90	−0.91	1.88
10	g^+	g^-	g^+			(absent)[f]			1.77

[a]In kcal mol^{-1}, relative to the all-trans conformation. [b]From E_model, at the MP2/6-311+G(2d,p)//B3LYP/6-311+G(2d,p) level. [c]From 1,2-dimethoxyethane, at the MP2/6-311++G(3df,3pd)//HF/6-31G(d) level.[30] [d]In the O−CH_2−CH_2−O bond sequence. [e]At the CH_2−CH_2 bond of the central unit of triglyme.[30] [f]Local minimum of the potential was not found by the geometrical optimization.

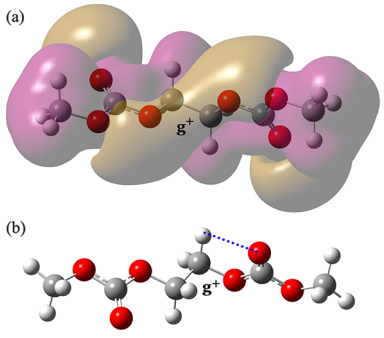

Figure 6. E_model: (a) tg^+t, electrostatic potential distribution and (b) ttg^+, an intramolecular C═O···H−C close contact (dotted line) with the O···H distance of 2.40 Å.

and is related to that ($(\Delta S)_p$) at constant pressure and that (ΔS_v) due to the volume change (ΔV) by[40,41]

$$S_{conf} = (\Delta S)_p - \Delta S_v \quad (3)$$

where $\Delta S_v = (\alpha/\beta)\Delta V$ with α and β being the thermal expansion coefficient and isothermal compressibility, respectively. The $S_{conf}/(\Delta S)_p$ ratio has been estimated as, for example, 0.8−0.9 for polyethers and polythioethers[42] and 0.5−0.7 for polyesters,[27] while amorphous elastomers exhibit comparatively small $S_{conf}/(\Delta S)_p$ values such as 0.5 (natural rubber) and 0.6 (gutta percha).[41] Therefore, amorphous PEC and PPC would also have somewhat smaller $S_{conf}/(\Delta S)_p$ ratios than those of semicrystalline polymers.

The characteristic ratios of the PPC chains with different regio- and stereosequences were also calculated. Then, the ΔG_k values on the chloroform solution were employed because the dielectric constant (ca. 3) of PPC[43] is comparatively close to that (4.8) of chloroform; the RIS calculations are expected to represent the amorphous PPC chain. According to the Bernoulli trial, the $\langle r^2\rangle_0/nl^2$ value of the infinite PPC chain (degree of polymerization $x = \infty$) was calculated as a function of p_{ortho} and p_R, as shown in Figure 7a. The p_{ortho} and p_R values change at an interval of 0.1. The stereoinversion ($(R) \rightarrow (S)$ or $(S) \rightarrow (R)$) and regioinversion ($(O) \rightarrow (A)$ or $(A) \rightarrow (O)$) were assumed to occur independently of each other (the independent-event model). In the Bernoulli trial, the calculated quantities $f(p)$'s always satisfy $f(p_{ortho}) = f(1 - p_{ortho})$ and $f(p_R) = f(1 - p_R)$ (see Table S3, Supporting Information); thus, the $f(p)$ is symmetric with respect to $p_{ortho} = 0.5$ and $p_R = 0.5$. The average of $f(p_{ortho})$ and $f(1 - p_{ortho})$ is given in Table 8. Similarly, in the Markov process, such symmetries were considered, and the average values were adopted.

In Figure 7a, therefore, the $\langle r^2\rangle_0/nl^2$ value is plotted within ranges of $0.0 \le p_{ortho} \le 0.5$ and $0.0 \le p_R \le 0.5$. When $p_R = 0.0$ (isotactic), the characteristic ratio increases from 2.26 to 2.66 with increasing p_{ortho}. In the range of $p_R = 0.4$−0.5 (atactic), the plotted data overlap each other at $\langle r^2\rangle_0/nl^2 \approx 2.54$; the stereochemically irregular PPC chains have almost the same average dimension independently of the regioregularity. It should be noted that the Bernoulli trial cannot generate the syndiotactic chain.

Most of the synthesized PPC chains keep the chirality of propylene oxide and include the H−T linkage predominantly. However, propylene oxide rarely undergoes abnormal ring-opening, and consequently, the PPC chain randomly includes adjoining H−H and T−T linkages, between which the chiral form is different from those of the neighbors;[14,21] therefore, both stereoinversion $(R) \rightarrow (S)$ or $(S) \rightarrow (R)$ and regioinversion $(O) \rightarrow (A)$ or $(A) \rightarrow (O)$ occur simultaneously. However, the probability of the defect stays as small as several percent. Thus, the configuration of the PPC chain with the defects may be represented by the Bernoulli trial in which both regio- and stereoinversions are synchronized (the synchronous model). In Figure 7b, the characteristic ratios thus calculated are plotted as a function of p_R ($=p_{ortho}$). The plot is also symmetric with respect to $p_R = 0.5$ and $p_{ortho} = 0.5$. The curve can be seen to decrease gradually with an increase in p_R; the synchronous inversions tend to render the PPC chain more contracted. However, the change in $\langle r^2\rangle_0/nl^2$ between $p_R = 0.0$ and 0.5 is ca. 10%.

In Figure 8a, the $\langle r^2\rangle_0/nl^2$ values calculated according to the Markov process are shown as a function of p_{H-T} and p_{meso}. Then, the p_{H-T} and p_{meso} values were changed from zero to unity at intervals of 0.1, and the contour lines in Figure 8 were drawn by interpolating the two-dimensional data meshes. In $p_{meso} = 0.0$ (syndiotactic), the $\langle r^2\rangle_0/nl^2$ value increases from 1.98 to 2.80 with increasing p_{H-T}, whereas, in $p_{meso} = 1.0$ (isotactic), it decreases from 3.08 to 2.26. Therefore, its maximum can be found at $p_{meso} = 1.0$ and $p_{H-T} = 0.0$: either (O,R)- and (A,R)-units or (O,S)- and (A,S)-units are arranged alternately. The minimum $\langle r^2\rangle_0/nl^2$ (≈2.0) is essentially equal to that (≈2.0) of the above synchronous model of $p_R = p_{ortho} = 0.5$ and located at the origin, $p_{meso} = p_{H-T} = 0.0$, where either (O,R)- and (A,S)-

DOI: 10.1021/acsomega.7b00964
ACS Omega 2017, 2, 4808−4819

Table 6. Conformer Free Energies (ΔG_k's) of PPC and Poly(propylene oxide) (PPO), Evaluated by Ab Initio MO Calculations[a]

				PPC[b]					PPO[c]
k	conformation[d]			gas	chloroform	acetone	methanol	DMSO	gas
1	t	t	t	0.00	0.00	0.00	0.00	0.00	0.00
2	t	t	g^+	2.22	2.36	2.41	2.42	2.42	3.20
3	t	t	g^-	−0.15	−0.18	−0.18	−0.18	−0.18	0.43
4	t	g^+	t	−0.47	−1.07	−1.31	−1.34	−1.36	0.62
5	t	g^+	g^+	2.28	1.82	1.58	1.55	1.53	3.80
6	t	g^+	g^-			(absent)[e]			−0.20
7	t	g^-	t	−0.06	−0.58	−0.84	−0.88	−0.90	1.57
8	t	g^-	g^+	5.06	4.32	3.91	3.85	3.82	2.18
9	t	g^-	g^-	−0.22	−0.70	−0.95	−0.98	−1.00	1.38
10	g^+	t	t			(absent)[e]			(absent)[e]
11	g^+	t	g^+			(absent)[e]			(absent)[e]
12	g^+	t	g^-			(absent)[e]			(absent)[e]
13	g^+	g^+	t	−0.78	−1.22	−1.39	−1.42	−1.43	2.30
14	g^+	g^+	g^+	2.02	2.02	2.01	2.00	2.00	4.02
15	g^+	g^+	g^-	2.19	1.13	0.69	0.62	0.59	1.34
16	g^+	g^-	t			(absent)[e]			0.99
17	g^+	g^-	g^+			(absent)[e]			(absent)[e]
18	g^+	g^-	g^-	−0.59	−0.78	−0.90	−0.92	−0.93	1.51
19	g^-	t	t	0.12	0.18	0.20	0.20	0.20	1.25
20	g^-	t	g^+	2.64	2.86	2.91	2.92	2.92	4.46
21	g^-	t	g^-			(absent)[e]			1.87
22	g^-	g^+	t			(absent)[e]			0.80
23	g^-	g^+	g^+	2.28	2.12	1.98	1.96	1.95	4.28
24	g^-	g^+	g^-			(absent)[e]			(absent)[e]
25	g^-	g^-	t	0.33	−0.11	−0.34	−0.37	−0.39	(absent)[e]
26	g^-	g^-	g^+	5.14	4.73	4.48	4.44	4.42	(absent)[e]
27	g^-	g^-	g^-	0.13	−0.13	−0.27	−0.29	−0.30	(absent)[e]

[a]In kcal mol^{-1}, relative to the all-trans conformation. [b]From (*R*)-P_model, at the MP2/6-311+G(2d,p)//B3LYP/6-311+G(2d,p) level. [c]From (*R*)-1,2-dimethoxypropane, at the MP2/6-31+G(d)//HF/6-31G(d) level.[31] [d]In the O−CH_2−CH(CH_3)−O bond sequence. [e]Local minimum of the potential was not found by the geometrical optimization.

Table 7. Bond Conformation of (*R*)-P_Model, Evaluated from MO Calculations

		bond 4			bond 5			bond 6		
medium	temp (°C)	p_t	p_{g^+}	p_{g^-}	p_t	p_{g^+}	p_{g^-}	p_t	p_{g^+}	p_{g^-}
gas	15	0.44	0.42	0.14	0.19	0.39	0.42	0.60	0.01	0.39
	25	0.45	0.41	0.14	0.20	0.38	0.42	0.59	0.01	0.40
	35	0.45	0.40	0.15	0.20	0.38	0.42	0.59	0.01	0.40
	45	0.45	0.40	0.15	0.21	0.37	0.42	0.59	0.01	0.40
	55	0.46	0.39	0.15	0.21	0.37	0.42	0.59	0.01	0.40
chloroform	15	0.49	0.41	0.10	0.10	0.49	0.41	0.67	0.00	0.33
	25	0.49	0.40	0.11	0.11	0.48	0.41	0.67	0.00	0.33
	35	0.49	0.40	0.11	0.11	0.48	0.41	0.66	0.01	0.33
	45	0.49	0.39	0.12	0.11	0.47	0.42	0.65	0.01	0.34
	55	0.49	0.39	0.12	0.12	0.46	0.42	0.65	0.01	0.34
acetone	15	0.51	0.39	0.10	0.07	0.51	0.42	0.68	0.00	0.32
	25	0.51	0.39	0.10	0.08	0.50	0.42	0.68	0.00	0.32
	35	0.51	0.38	0.11	0.08	0.49	0.43	0.67	0.01	0.32
	45	0.51	0.38	0.11	0.09	0.48	0.43	0.67	0.01	0.32
methanol	15	0.51	0.39	0.10	0.07	0.51	0.42	0.69	0.00	0.31
	25	0.52	0.38	0.10	0.07	0.50	0.43	0.68	0.00	0.32
	35	0.52	0.38	0.10	0.08	0.49	0.43	0.67	0.01	0.32
	45	0.52	0.37	0.11	0.08	0.48	0.44	0.67	0.01	0.32
	55	0.52	0.37	0.11	0.08	0.48	0.44	0.66	0.01	0.33
DMSO	25	0.52	0.38	0.10	0.07	0.50	0.43	0.68	0.00	0.32
	35	0.52	0.38	0.10	0.08	0.49	0.43	0.67	0.01	0.32
	45	0.52	0.37	0.11	0.08	0.48	0.44	0.67	0.01	0.32
	55	0.52	0.37	0.11	0.08	0.48	0.44	0.66	0.01	0.33

DOI: 10.1021/acsomega.7b00964
ACS Omega 2017, 2, 4808−4819

Table 8. Configurational Properties and Averaged Geometrical Parameters of PEC and Isotactic (*R*)-PPC at 25 °C, Evaluated from the Refined RIS Calculations with MO Parameters Including Solvent Effects

		gas	chloroform	acetone	methanol	DMSO
			PEC			
$\langle r^2\rangle_0/nl^2$		2.42	2.52	2.54	2.54	2.54
$d\ln\langle r^2\rangle_0/dT \times 10^3$ (K^{-1})		0.32	−0.12	−0.25	−0.26	−0.27
S_{conf} (cal K^{-1} mol^{-1})		5.51	5.16	4.97	4.94	4.93
$f_U/f \times 10^3$		95	−35	−73	−78	−80
geometry[a] (chloroform)	bond	$\bar{l}$	$\bar{\theta}$	$\bar{\phi}_t$	$\bar{\phi}_{g^+}$	$\bar{\phi}_{g^-}$
	a	1.339	107.9	0.0		
	b	1.339	115.5	0.0		
	c	1.440	110.0	0.0	95.5	−95.5
	d	1.510	110.0	0.0	111.9	−111.9
	e	1.440	115.5	0.0	95.5	−95.5
		gas	chloroform	acetone	methanol	DMSO
			Isotactic (*R*)-PPC of 100% H−T			
$\langle r^2\rangle_0/nl^2$		2.36	2.26	2.26	2.26	2.26
$d\ln\langle r^2\rangle_0/dT \times 10^3$ (K^{-1})		1.07	0.44	0.24	0.20	0.18
S_{conf} (cal K^{-1} mol^{-1})		4.34	4.12	4.05	4.04	4.03
$f_U/f \times 10^3$		320	130	72	60	52
geometry[a] (chloroform)	bond	$\bar{l}$	$\bar{\theta}$	$\bar{\phi}_t$	$\bar{\phi}_{g^+}$	$\bar{\phi}_{g^-}$
	a	1.337	107.9	0.0		
	b	1.340	115.5	−0.1		
	c	1.440	110.1	0.1	87.7	−72.3
	d	1.517	107.3	3.4	111.9	−113.0
	e	1.453	116.5	−31.0	116.5	−96.8

[a]Geometrical parameters averaged at 25 °C with the MO energies on the chloroform solution. Symbols: $\bar{l}$, averaged bond length (in Å); $\bar{\theta}$, averaged bond angle (in deg); $\bar{\phi}_\xi$, average dihedral angle (in deg) of the ξ conformation.

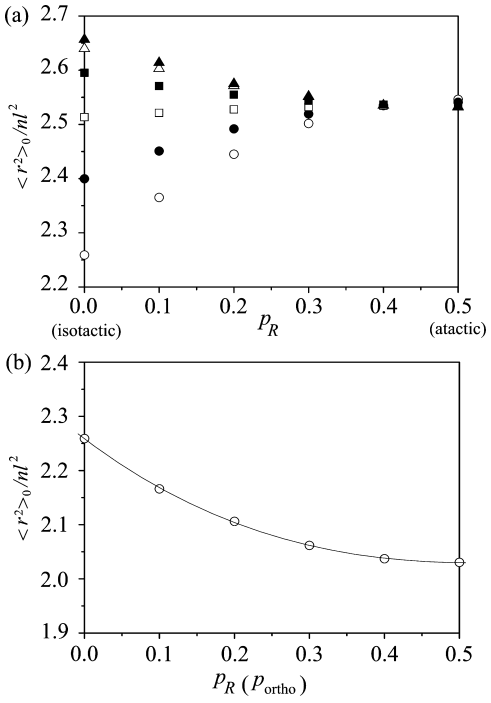

Figure 7. Characteristic ratios ($\langle r^2\rangle_0/nl^2$'s) of PPC, derived from the refined RIS calculations with the Bernoulli trial. (a) (Independent-event model) the regio- and stereosequences were generated independently of each other, and the $\langle r^2\rangle_0/nl^2$' values are plotted against p_R for different p_{ortho} and (p_{H-T}, p_{H-H}, p_{T-T}) values: 0.0 and (1.00, 0.00, 0.00) (open circle); 0.10 and (0.82, 0.09, 0.09) (filled circle); 0.20 and (0.68, 0.16, 0.16) (open square); 0.30 and (0.58, 0.21, 0.21) (filled square); 0.40 and (0.52, 0.24, 0.24) (open triangle); and 0.50 and (0.50, 0.25, 0.25) (filled triangle). (b) (Synchronous model) the regio- and stereoforms are changed synchronously: (*O*,*R*) → (*A*,*S*), (*A*,*R*) → (*O*,*S*), (*O*,*S*) → (*A*,*R*), or (*A*,*S*) → (*O*,*R*). The solid line represents a cubic function fitted to the calculated date (open circle).

units or (*A*,*R*)- and (*O*,*S*)-units are arranged alternately (the synchronous inversions).

Characteristics of the Polycarbonate Chains. It is known that PEO crystallizes in the tgt conformation.[44] As our MO calculations indicate, PEC is also most stabilized in this conformation. Nevertheless, PEC is an amorphous polymer. Figure 6a shows the charge distribution of E_model whose O−CH_2−CH_2−O bonds lie in the tgt state. The carbonate group with three oxygen atoms draws electrons, and the negative charge appears to be distributed helically on the molecular surface. Accordingly, the PEC chains repel each other and fail to form a regular packing. This may be an origin of its amorphous nature. In addition, as shown above, PEC and PPC strongly prefer distorted conformations including a number of gauche bonds. This is also an origin.

For liquid crystalline polycarbonates, the geometrical characters of the carbonate linkage were revealed.[45] The O−C(=O)−O group lies on a plane, and the O−C−O and C(=O)−O−C angles were determined to be 108° and 118.3°, respectively; therefore, the mesogenic cores can scarcely be arranged in parallel with each other, and hence this structural distortion affects the stability of the liquid crystalline phase. The present study has evaluated bond angles of bonds a and b of PEC and PPC to be 107.9° and 115.5°, respectively (Table 8). In these two polycarbonates, therefore, the linearity of the chain backbone would be unattainable even though they were in the all-trans form. This may also be a reason for their amorphous nature.

Inasmuch as amorphous PEC and PPC chains lie in near unperturbed states, the refined RIS calculations can provide reliable insights into their solid-state properties as well as solution (melt) properties. Because of the distorted conformations, PEC and PPC exhibit the characteristic ratios smaller than those of common linear polymers. The RIS calculations with the Markov chain showed that the characteristic ratio of PPC does not depend significantly on the regio- and stereoregularities. The reason may be explained as follows. The carbonate group separates the neighboring rotatable O−CH_2−$CH(CH_3)$−O parts with two rigid O−C(=O)−O bonds; therefore, the conformational correlations can be only weakly transmitted to the adjacent monomeric unit, and hence the individual units are allowed to change the conformation nearly independently of the neighbors. As far as PPC is concerned, the regio- and stereoregularities have no significant effects on the spatial configuration and probably on the other physical properties.

Mechanical Properties. Flory et al. thermodynamically revealed the requirement for rubberlike elasticity of polymers.[46−51] On this basis, we can discuss whether amorphous PEC and PPC will exhibit rubberlike chain elasticity.

DOI: 10.1021/acsomega.7b00964
ACS Omega 2017, 2, 4808−4819

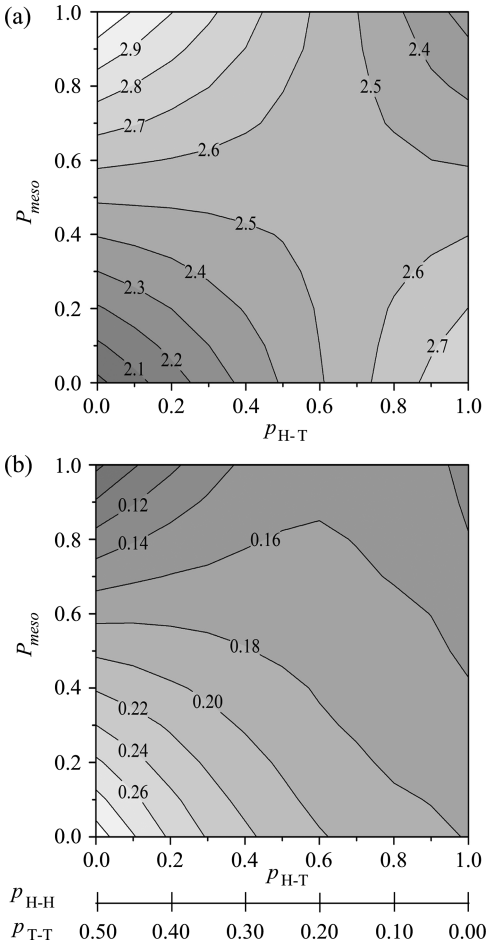

Figure 8. (a) $\langle r^2\rangle_0/nl^2$ and (b) f_U/f values (displayed numerically on the maps) of PPC with different regio- and stereosequences, derived from the refined RIS calculations with the Markov stochastic process and plotted as two-dimensional contour plots against p_{H-T} and p_{meso}.

The tension (f) of an elastomer is composed of two terms due to internal-energy (U) and entropy (S) changes[46]

$$f = f_U + f_S \tag{4}$$

where

$$f_U = \left(\frac{\partial U}{\partial L}\right)_{T,V} \tag{5}$$

and

$$f_S = -T\left(\frac{\partial S}{\partial L}\right)_{T,V} \tag{6}$$

with T, V, and L being the absolute temperature, volume, and length, respectively. The f_U/f ratio is expressed as a function of the temperature coefficient of the mean square end-to-end distance by[47−50]

$$\frac{f_U}{f} = -T\left[\frac{\partial \ln(f/T)}{\partial T}\right]_{L,V} = T\frac{\mathrm{d}\ln\langle r^2\rangle_0}{\mathrm{d}T} \tag{7}$$

Although intermolecular interactions occur in rubberlike materials, these interactions have been assumed to be independent of the configurations of the network chains. In other words, it is well-established that rubberlike elasticity is principally of intramolecular origin.[48,50,52] Therefore, we are allowed to discuss the possibility that the two polycarbonates will act as elastomers, on the basis of eq 7, which can be evaluated from the refined RIS calculations.

The f_U/f ratios of PEC and isotactic PPC of 100% H−T linkage at 25 °C were evaluated from the $\mathrm{d}\ln\langle r^2\rangle_0/\mathrm{d}T$ values (in Table 8). The PEC chain has a positive value of 0.095 in the gas phase but negatives of −0.035 to −0.080 in the solvents, whereas PPC always shows positive values (0.32−0.052). For both polycarbonates, the f_U/f ratio tends to decrease with increasing medium polarity. The sign of f_U/f can be related to conformational changes during chain deformation as follows.

It is known that polyethylene shows negative f_U/f values of ca. −0.4.[47,49,50] Its CH_2-CH_2 bond prefers the trans conformation, and the trans-gauche energy difference is 0.4−0.5 kcal mol^{-1}.[35,53] As temperature increases ($\Delta T > 0$), the trans conformations partly change to distorted gauche states of higher energy, and hence the chain dimension decreases ($\Delta\langle r^2\rangle_0 < 0$, $\Delta L < 0$, and $\Delta U > 0$), accordingly, $\mathrm{d}\ln\langle r^2\rangle_0/\mathrm{d}T < 0$, $\Delta U/\Delta L \approx (\partial U/\partial L) < 0$, and $f_U/f < 0$. The negative f_U/f works against the entropic elasticity because the f_S term must always be positive.

The PPC chain gives positive f_U/f values. This is because, in contrast to polyethylene, PPC by nature chooses distorted conformations such as g^+g^+t, $g^+g^-g^-$, tg^+t, tg^-g^-, and tg^-t. As the temperature is increased, the distortion is released by the gauche-to-trans change, and hence, the chain is extended: $\mathrm{d}\ln\langle r^2\rangle_0/\mathrm{d}T > 0$. The stretching (contraction) of the PPC chain increases (decreases) the internal energy: $(\partial U/\partial L) > 0$, therefore, $f_U/f > 0$. The conformational characteristic of PPC supports its entropic elasticity. On the other hand, PEC changes the sign of f_U/f, depending on the surroundings. It is well-known that elastomers give positive f_U/f values: *cis*-1,4-polybutadiene (0.10−0.17), polydimethylsiloxane (0.13−0.30), and natural rubber (0.12−0.18).[50] Therefore, the PPC chain may be more likely than PEC to behave as an elastomer.

The f_U/f ratios of PPC were calculated according to the Markov model as a function of p_{H-T} and p_{meso}. In Figure 8b, the data are also plotted as a two-dimensional contour map. The maximum f_U/f value (0.311) is found at the origin ($p_{H-T} = p_{meso} = 0$), where the minimum characteristic ratio was predicted above, and the PPC chain is a perfect alternating copolymer of either (*O*,*R*)- and (*A*,*S*)-monomers or (*O*,*S*)- and (*A*,*R*)-monomers. The minimum f_U/f (0.075) is indicated to be located at the left top corner ($p_{H-T} = 0$ and $p_{meso} = 1$), where the maximum $\langle r^2\rangle_0/nl^2$ was suggested, and the PPC chain is an alternating copolymer of either (*O*,*R*)- and (*A*,*R*)-units or (*O*,*S*)- and (*A*,*S*)-units. These facts suggest an inverse correlation between f_U/f and $\langle r^2\rangle_0/nl^2$, that is, between the rubberlike elasticity and the chain dimension.

It has been reported that PEC with a low T_g of ca. 10 °C behaves as an elastomer at room temperature with an elongation at break greater than 600% and completely recovers to the initial length after removal of the load.[54] On the other hand, mechanical properties of PPC are more complicated owing to its higher T_g of 35−42 °C. Although PPC is brittle below 20 °C, an effective plasticizer (10 wt % of 1,6-bis(methyl urethane)hexane) was found to reduce T_g of PPC significantly and improve the mechanical properties: elongation at break, ca. 700% and tensile strength, 30 MPa.[55] In addition, PPC was mixed with rubbery polyurethane particles (30 wt %) to show an impact strength of as much as 228.3 J m^{-1}.[56] When amorphous PPC was blended and fixed by graft polymerization

DOI: 10.1021/acsomega.7b00964
ACS Omega 2017, 2, 4808−4819

with poly(β-hydroxybutyrate-*co*-hydroxyvalerate) (PHBV) (PHBV/PPC = 30:70 in weight), the composite materials exhibited a marked elongation at break of 1300%.[57] In addition, block copolymers of PPC with poly(ethylene glycol), having weight-average molecular weights of 81 000 and 225 000, were shown to be stretchable up to 870 and 720%, respectively, even though the PPC alone was so brittle as to be broken at only a 7% extension.[58] Accordingly, effective processing such as copolymerization, cross-linking, blending, and plasticizing for PEC and PPC will reveal their potential mechanical properties.

On Applications of PEC and PPC. Another expectable utilization of PEC and PPC is ion-conductive polymer electrolytes. As a representative polymer for this purpose, we can mention PEO. It is known that PEO is capable of changing the conformational preference according to the environment.[29,30,59] In the gas phase or nonpolar media, the energy difference between ttt and tgt states in the O−CH_2−CH_2−O bonds is close to null. In polar solvents, however, the tgt conformation will be more stable than ttt by over 1.0 kcal mol^{-1}. As found for crown ethers,[60] the PEO chain adopts the tgt conformation and captures a cation such as alkali metal ions. Inasmuch as PEO is semicrystalline, the cations will be trapped only in the amorphous phase and on the crystallite surface. The ionic conductivity of PEO is reported to be on the order of 10^{-8} to 10^{-7} S cm^{-1}.[61]

The present study has shown that the tg^+t and tg^+g^+ conformations of PEC are more stable in ΔG_k than those of PEO. Therefore, the O−CH_2−CH_2−O bond sequence as well as the electronegative carbonate group (see Figure 6a) can readily capture, for example, Li^+ ion. In addition, PEC and PPC are completely amorphous, and hence most monomeric units are ready to accept Li^+ ions. Compared with PEO, therefore, PEC can interact with much more inorganic salts, and its ionic conductivity is as high as ∼10^{-4} S cm^{-1}.[61,62] As can be seen from Table 6, stable conformations in the O−CH_2−C*H-(CH_3)−O bond sequence of P_model are tg^+t, g^+g^+t, tg^-g^-, and $g^+g^-g^-$, and hence amorphous PPC can also capture Li^+ ion effectually. For a PPC/$Li_{6.76}La_3Zr_{1.75}Ta_{0.25}O_{12}$ composite, the following electric characteristics have been reported: ionic conductivity, 5.2 × 10^{-4} S cm^{-1}; electrochemical window, 4.6 V; and ionic transference number, 0.75.[63] The green polymers produced from carbon dioxide would be future ion-conductive electrolytes to illuminate the world.

CONCLUSIONS

Conformational characteristics and configurational properties of PEC and PPC have been elucidated by the methodology based on MO calculations, NMR experiments, and RIS calculations. Both PEC and PPC were found to strongly prefer distorted conformations including a number of gauche states. In the RIS calculations on PPC, the Bernoulli and Markov stochastic processes were employed to generate its regio- and stereosequences, and its configurational properties were shown not to depend significantly on the regio- and stereosequences. The physical properties, practical uses, and potential applications of the two polycarbonates have been discussed in terms of the structural information thus obtained. In conclusion, as a result of the detailed computational characterization, it is preferable that PEC and PPC should be prepared at low costs so as to give high yields without paying particular attention to the regio- and stereoregularities, processed so as to lower the glass transition temperatures, and used as high-value added flexible functional materials.

METHODS

Synthesis of Model Compounds. Methyl chloroformate (9.7 mL, 0.125 mol), dissolved in chloroform (12.5 mL), was added dropwise under argon atmosphere to ethylene glycol (2.8 mL, 0.05 mol) and pyridine (20 mL), and the mixture was stirred at 0 °C for 3 h and then at room temperature overnight.[64] The reaction mixture was acidified to pH = 2 with hydrochloric acid (20 mL) and underwent extraction twice with chloroform (15 mL × 2). The organic layer was washed thrice with saturated solution of sodium bicarbonate (30 mL × 3) and dried over anhydrous sodium sulfate (ca. 10 g) overnight. The solution was filtrated and condensed on a rotary evaporator. The residue was dried in vacuo at 35 °C for 3 h to yield ethylene glycol bis(methyl carbonate) (E_model) (yield, 86%).

Propylene glycol bis(methyl carbonate) (P_model) was synthesized similarly except that propylene glycol was used instead of ethylene glycol. The yield was 50%.

NMR Measurements. Proton NMR spectra were recorded at 500 MHz on a JEOL JNM-ECA500 spectrometer in the Center for Analytical Instrumentation of Chiba University. The sample temperature was increased stepwise from 15 or 25 °C to 45 or 55 °C at intervals of 10 °C. Free induction decays (FIDs) were accumulated under the following conditions: scan, 32−128; 45° pulse width, 5.7 μs; acquisition time, 4.4 s; and recycle delay, 4 s. The FID was fully zero-filled prior to the Fourier transform to yield enough digital resolution in Hz for the subsequent analysis. The NMR solvents were chloroform-*d*, acetone-d_6, methanol-d_4, and dimethyl-d_6 sulfoxide (DMSO-d_6), and 5 mm NMR sample tubes were used. The obtained spectra were simulated with the gNMR program[65] to yield ^{1}H chemical shifts and ^{1}H−^{1}H coupling constants.

NMR Analysis. Vicinal ^{1}H−^{1}H coupling constants (J_{HH} and J'_{HH}) observed from the methylene protons, A, A′, B, and B′ of E_model (see Figures 4 and 9) can be expressed as weight averages of J_T's and J_G's

$$J_{HH} = J_{AB} = J_{A'B'} = J_G p_t + \frac{J'_T + J'_G}{2} p_g \tag{8}$$

and

$$J'_{HH} = J_{A'B} = J_{AB'} = J_T p_t + J''_G p_g \tag{9}$$

where the weights, p_t and p_g, are trans and gauche fractions of the CH_2−CH_2 bond, respectively. By definition, we have

$$p_t + p_g = 1 \tag{10}$$

where $p_{g^+} = p_{g^-} = p_g/2$.

There is the possibility that P_model is either (*R*)- or (*S*)-isomer, but both give the identical NMR spectra. Therefore, although we employed its racemic mixture in NMR measurements, we are allowed to analyze the observed spectra with either isomeric model. Herein, the (*R*)-P_model is used throughout. Vicinal coupling constants between the methylene (A or B) and methine (C) protons are expressed as

$$J_{AC} = J_G p_t + J'_T p_{g^+} + J''_G p_{g^-} \tag{11}$$

and

$$J_{BC} = J_T p_t + J'_G p_{g^+} + J'''_G p_{g^-} \tag{12}$$

For J_T's and J_G's, see Figure 9. The trans, gauche$^+$, and gauche$^-$ fractions fulfill

DOI: 10.1021/acsomega.7b00964
ACS Omega 2017, 2, 4808−4819

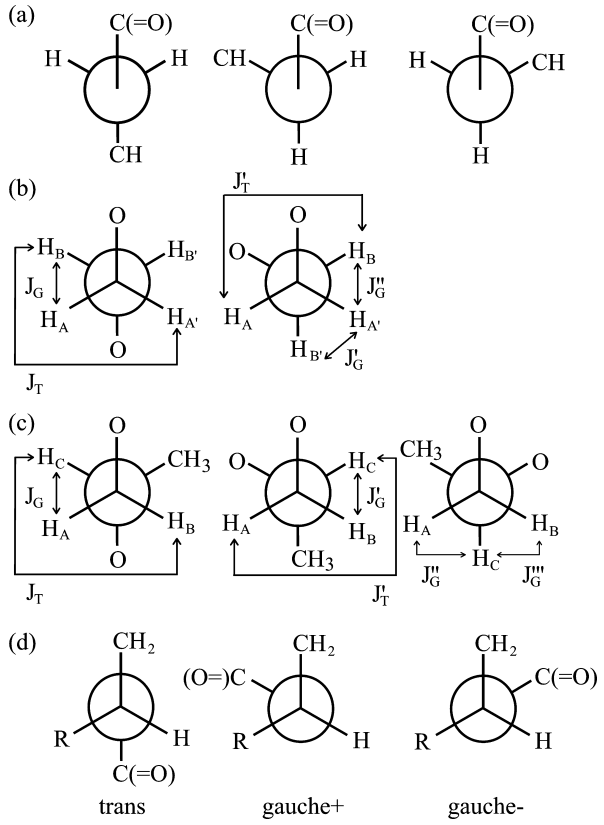

Figure 9. Rotamers around bonds (a) 4 of E_model and P_model, (b) 5 of E_model, (c) 5 of (*R*)-P_model, and (d) 6 of E_ (*R* = H) and (*R*)-P_ (*R* = CH_3) models. For the bond numbers, see Figure 4. The vicinal J_T and J_G couplings used in eqs 8, 9, 11, and 12 are defined as illustrated.

$$p_t + p_{g^+} + p_{g^-} = 1 \tag{13}$$

It should be noted that the gauche$^+$ and gauche$^-$ states are not equivalent: $p_{g^+} \neq p_{g^-}$. Substitution of the observed *J* values into the above equations yields p_t and p_g of E_model or p_t, p_{g^+}, and p_{g^-} of P_model, if the J_T and J_G values are given beforehand. This study has adopted two sets of J_T and J_G: set A, J_T's = 9.87 and J_G's = 2.54 Hz for the chloroform solution and J_T's = 10.25 and J_G's = 2.52 Hz for the acetone, methanol, and DMSO solutions (taken from those of *cis*-2,6-dimethyl-1,4-dioxane[66]); set B, J_T's = 11.4 and J_G's = 2.3 Hz (optimized for 1,2-dimethoxyethane[28]).

Molecular Orbital Calculations. MO calculations on the model compounds were carried out with the Gaussian 09 program[67] installed on an HPC Systems 5000-Z800 computer. For each conformer, the molecular geometry was fully optimized at the B3LYP/6-311+G(2d,p) level under the tight convergence, and thermochemical energies at 25 °C and 1 atm were also computed by the frequency calculation at the same level. Furthermore, the electronic energy was calculated at the MP2/6-311+G(2d,p) level for the optimized geometry. The conformer free energy was obtained from the MP2 electronic energy and the B3LYP thermochemical correction term to the Gibbs free energy, being expressed as the difference (ΔG_k, *k*: conformer) from that of the all-trans conformation. The solvent effect on the MP2 electronic energy was evaluated by the polarizable continuum model using the integral equation formalism variant.[68]

Rotational Isomeric State Calculation. The *refined* RIS scheme[23,35,69] was applied to PEC and PPC. The refined RIS scheme has been developed so as to change both conformational energy and geometrical parameters with conformations of the neighboring as well as current bonds to yield accurate results. The statistical weight matrices of PEC and PPC were formulated on the basis of the chemical structures shown in Figure 1 and as presented in Appendices A and B (Supporting Information). The geometrical parameters of PEC and PPC were chosen from the optimized structures of E_model and P_model, respectively, being tabulated in Tables S1 and S2 (Supporting Information).

Conventionally, the C*H(CH_3) and CH_2 parts of PPC have been termed *head* and *tail*, respectively. Herein, the CH_2 → C*H(CH_3) (tail → head) and C*H(CH_3) → CH_2 (head → tail) directions are designated as orthodromic (*O*) and antidromic (*A*), respectively (see Figure 3). However, this definition is not absolute: if the (*O*)-isomer is turned around 180° with respect to a line perpendicular to the chain axis, it becomes the (*A*)-isomer. Nevertheless, the RIS scheme requires us to determine the moving direction for the matrix multiplication. For example, when the monomer (propylene oxide + carbonate) has the *O* direction and (*R*)-chiral center, it is represented herein as (*O*,*R*)-monomer. The *OO*, *OA*, *AA*, and *AO* combinations between monomers form H−T, H−H, T−H, and T−T linkages, respectively, as illustrated in Figure 3. Inasmuch as the H−T and T−H linkages are identical, the regiosequences expressed in the *O* and *A* manner can be rewritten in terms of H−T, H−H, and T−T.

If we obtain conformer free energies of (*O*,*R*)-monomer of PPC and formulate its statistical weight matrices U_j's (*j*: bond number), we can derive U_j's of (*O*,*S*)-, and (*A*,*R*)-, and (*A*,*S*)-monomers by proper matrix operations as shown in Appendix B (Supporting Information). From the optimized geometrical parameters of (*O*,*R*)-monomer (Table S2, Supporting Information), we can also derive those of the other three isomers.

To arrange the stereo- and regiosequences of the PPC chain, we have adopted two stochastic processes: the Bernoulli trial and the first-order Markov chain.[24,25] In the Bernoulli trial, a random number was generated between zero and unity. When the number was smaller than or equal to the given p_R value, the next repeating unit was (*R*)-isomer. Otherwise, (*S*)-isomer was selected. Here, p_R represents the (*R*)-isomeric probability. The regiosequences were determined similarly with the *O* probability (p_{ortho}) instead of p_R. The operation was repeated up to a given degree (*x*) of polymerization over a given number (n_c) of chains. Fractions of the regio- (H−T, H−H, and T−T) and stereosequences (diad, *meso*, and *racemo*; triad, *mm*, *mr*, *rm*, and *rr*) were calculated as a function of p_R and p_{ortho}, according to the Bernoulli trial as given in Table S3 (Supporting Information).

In the Markov process, a random number was generated within the range of zero to unity. When the value was smaller or equal to p_{meso} (or p_{H-T}), the same optical isomer (direction) as that of the preceding monomer was added. Otherwise, the other isomer (orientation) was added. Here, p_{meso} and p_{H-T} are probabilities of *meso* diad and H−T linkage, respectively. This operation was repeated $x \times n_c$ times as above. Fractions of the regio- and stereosequences based on the Markov chain are also listed in Table S3 (Supporting Information).

In accordance with the stereo- and regiosequences of the PPC chains thus generated, the super generator matrices H_β^α's

DOI: 10.1021/acsomega.7b00964
ACS Omega 2017, 2, 4808−4819

(α = R or S and β = O or A)[23] were chosen, arranged, and multiplied sequentially to yield the configurational properties and thermodynamic quantities for the individual chains. The final outcomes were the averages over all of the n_c chains. In our previous study on poly(lactide)s,[70] fluctuations in data resulting from the stochastic processes were found to decrease with increasing number ($x \times n_c$) of trials. When $x = n_c = 300$, the accuracy and reproducibility were fully satisfactory. Therefore, this study has generally employed $x = n_c = 300$, except when the data on the infinite chain ($x = \infty$) were determined from the extrapolation of the datum versus x^{-1} plot. Then, the x and n_c values were set as $100 \leq x \leq 300$ and $n_c = 300$.

■ ASSOCIATED CONTENT

Supporting Information

The Supporting Information is available free of charge on the ACS Publications website at DOI: 10.1021/acsomega.7b00964.

Statistical weight matrices of PEC; statistical weight matrices of PPC; geometrical parameters of PEC; geometrical parameters of PPC; and fractions of reigo- and stereosequences in Bernoulli and Markov statistics for PPC (PDF)

■ AUTHOR INFORMATION

Corresponding Author

*E-mail: sasanuma@faculty.chiba-u.jp. Phone: +81 (0)43 290 3394. Fax: +81 (0)43 290 3394.

Notes

The authors declare no competing financial interest.

■ ACKNOWLEDGMENTS

This study was partially supported by the Grants-in-Aid for Scientific Research (C) (16K05906) from the Japan Society for the Promotion of Science.

■ REFERENCES

(1) Patrick, S. G. *Practical Guide to Polyvinyl Chloride*; Rapra Technology: Shawbury, U.K., 2005; Chapter 2.

(2) Inoue, S.; Koinuma, H.; Tsuruta, T. Copolymerization of carbon dioxide and epoxide. *J. Polym. Sci., Part B: Polym. Lett.* **1969**, *7*, 287−292.

(3) Inoue, S.; Koinuma, H.; Tsuruta, T. Copolymerization of carbon dioxide and epoxide with organometallic compounds. *Makromol. Chem.* **1969**, *130*, 210−220.

(4) Lin, Y.; Yan, Q.; Kong, C.; Chen, L. Polyethyleneimine incorporated metal-organic frameworks adsorbent for highly selective CO_2 capture. *Sci. Rep.* **2013**, *3*, 1859.

(5) Zhang, W.; Liu, H.; Sun, C.; Drage, T. C.; Snape, C. E. Capturing CO_2 from ambient air using a polyethyleneimine−silica adsorbent in fluidized beds. *Chem. Eng. Sci.* **2014**, *116*, 306−316.

(6) Sasanuma, Y.; Hattori, S.; Imazu, S.; Ikeda, S.; Kaizuka, T.; Iijima, T.; Sawanobori, M.; Azam, M. A.; Law, R. V.; Steinke, J. H. G. Conformational analysis of poly(ethylene imine) and its model compounds: rotational and inversional isomerizations and intramolecular and intermolecular hydrogen bonds. *Macromolecules* **2004**, *37*, 9169−9183.

(7) Fukuda, Y.; Abe, D.; Tanaka, Y.; Uchida, J.; Suzuki, N.; Miyai, T.; Sasanuma, Y. Solution properties of poly(*N*-methylethylene imine), a highly hydrophilic polycation. *Polym. J.* **2016**, *48*, 1065−1072.

(8) Sasanuma, Y.; Teramae, F.; Yamashita, H.; Hamano, I.; Hattori, S. Conformational analysis of poly(trimethylene imine) and poly(*N*-methyltrimethylene imine) by the rotational isomeric state scheme with up to fourth-order intramolecular interactions. *Macromolecules* **2005**, *38*, 3519−3532.

(9) Udipi, K.; Gillham, J. K. Poly(ethylene carbonate) and poly(propylene carbonate): Transitions and thermomechanical spectra. *J. Appl. Polym. Sci.* **1974**, *18*, 1575−1580.

(10) Chisholm, M. H.; Navarro-Llobet, D.; Zhou, Z. Poly(propylene carbonate). 1. More about poly(propylene carbonate) formed from the copolymerization of propylene oxide and carbon dioxide employing a zinc glutarate catalyst. *Macromolecules* **2002**, *35*, 6494−6504.

(11) Allen, S. D.; Moore, D. R.; Lobkovsky, E. B.; Coates, G. W. High-activity, single-site catalysts for the alternating copolymerization of CO_2 and propylene oxide. *J. Am. Chem. Soc.* **2002**, *124*, 14284−14285.

(12) Qin, Z.; Thomas, C. M.; Lee, S.; Coates, G. W. Cobalt-based complexes for the copolymerization of propylene oxide and CO_2: Active and selective catalysts for polycarbonate synthesis. *Angew. Chem., Int. Ed.* **2003**, *42*, 5484−5487.

(13) Quan, Z.; Min, J.; Zhou, Q.; Xie, D.; Liu, J.; Wang, X.; Zhao, X.; Wang, F. Synthesis and properties of carbon dioxide—epoxides copolymers from rare earth metal catalyst. *Macromol. Symp.* **2003**, *195*, 281−286.

(14) Chisholm, M. H.; Zhou, Z. Concerning the mechanism of the ring opening of propylene oxide in the copolymerization of propylene oxide and carbon dioxide to give poly(propylene carbonate). *J. Am. Chem. Soc.* **2004**, *126*, 11030−11039.

(15) Lu, X.-B.; Wang, Y. Highly active, binary catalyst systems for the alternating copolymerization of CO_2 and epoxides under mild conditions. *Angew. Chem., Int. Ed.* **2004**, *43*, 3574−3577.

(16) Coates, G. W.; Moore, D. R. Discrete metal-based catalysts for the copolymerization of CO_2 and epoxides: Discovery, reactivity, optimization, and mechanism. *Angew. Chem., Int. Ed.* **2004**, *43*, 6618−6639.

(17) Darensbourg, D. J. Making plastics from carbon dioxide: Salen metal complexes as catalysts for the production of polycarbonates from epoxides and CO_2. *Chem. Rev.* **2007**, *107*, 2388−2410.

(18) Luinstra, G. A. Poly(propylene carbonate), old copolymers of propylene oxide and carbon dioxide with new interests: Catalysis and material properties. *Polym. Rev.* **2008**, *48*, 192−219.

(19) Nakano, K.; Kobayashi, K.; Nozaki, K. Tetravalent metal complexes as a new family of catalysts for copolymerization of epoxides with carbon dioxide. *J. Am. Chem. Soc.* **2011**, *133*, 10720−10723.

(20) Nakano, K.; Hashimoto, S.; Nakamura, M.; Kamada, T.; Nozaki, K. Stereocomplex of poly(propylene carbonate): Synthesis of stereogradient poly(propylene carbonate) by regio- and enantioselective copolymerization of propylene oxide with carbon dioxide. *Angew. Chem., Int. Ed.* **2011**, *50*, 4868−4871.

(21) Salmeia, K. A.; Vagin, S.; Anderson, C. E.; Rieger, B. Poly(propylene carbonate): Insight into the microstructure and enantioselective ring-opening mechanism. *Macromolecules* **2012**, *45*, 8604−8613.

(22) Nakano, K.; Kobayashi, K.; Ohkawara, T.; Imoto, H.; Nozaki, K. Copolymerization of epoxides with carbon dioxide catalyzed by iron−corrole complexes: Synthesis of a crystalline copolymer. *J. Am. Chem. Soc.* **2013**, *135*, 8456−8459.

(23) Sasanuma, Y.; Asai, S.; Kumagai, R. Conformational characteristics and configurational properties of poly(ethylene oxide-*alt*-ethylene sulfide). *Macromolecules* **2007**, *40*, 3488−3497.

(24) Taylor, H. M.; Karlin, S. *An Introduction To Stochastic Modeling*, 3rd ed.; Academic Press: San Diego, 1998.

(25) Melsa, J. L.; Sage, A. P. *An Introduction To Probability & Stochastic Processes*; Dover Publications: Mineola, New York, USA, 2013.

(26) Sasanuma, Y. Conformational characteristics, configurational properties, and thermodynamic characteristics of poly(ethylene terephthalate) and poly(ethylene-2,6-naphthalate). *Macromolecules* **2009**, *42*, 2854−2862.

DOI: 10.1021/acsomega.7b00964
ACS Omega 2017, 2, 4808−4819

(27) Sasanuma, Y.; Nonaka, Y.; Yamaguchi, Y. Conformational characteristics and configurational properties of poly(ethylene succinate) and poly(butylene succinate) and structure−property−function relationships of representative biodegradable polyesters. *Polymer* **2015**, *56*, 327−339.
(28) Tasaki, K.; Abe, A. NMR studies and conformational energy calculations of 1,2-dimethoxyethane and poly(oxyethylene). *Polym. J.* **1985**, *17*, 641−655.
(29) Sasanuma, Y.; Ohta, H.; Touma, I.; Matoba, H.; Hayashi, Y.; Kaito, A. Conformational characteristics of poly(ethylene sulfide) and poly(ethylene oxide): Solvent dependence of attractive and repulsive gauche effects. *Macromolecules* **2002**, *35*, 3748−3761 , and references cited therein.
(30) Sasanuma, Y.; Sugita, K. The attractive gauche effect of ethylene oxides. *Polym. J.* **2006**, *38*, 983−988.
(31) Sasanuma, Y. Conformational analysis of poly(propylene oxide) and its model compound 1,2-dimethoxypropane. *Macromolecules* **1995**, *28*, 8629−8638 , and references cited therein.
(32) Abe, A.; Mark, J. E. Conformational energies and the random-coil dimensions and dipole moments of the polyoxides CH_3O-$[(CH_2)_yO]_xCH_3$. *J. Am. Chem. Soc.* **1976**, *98*, 6468−6476.
(33) Kawaguchi, S.; Imai, G.; Suzuki, J.; Miyahara, A.; Kitano, T.; Ito, K. Aqueous solution properties of oligo- and poly(ethylene oxide) by static light scattering and intrinsic viscosity. *Polymer* **1997**, *38*, 2885−2891.
(34) Allen, G.; Booth, C.; Price, C. III—The unperturbed dimensions of poly(propylene oxide). *Polymer* **1967**, *8*, 397−401.
(35) Flory, P. J. *Statistical Mechanics of Chain Molecules*; Wiley & Sons: New York, USA, 1969.
(36) Lieser, G.; Fischer, E. W.; Ibel, K. Conformation of polyethylene molecules in the melt as revealed by small-angle neutron scattering. *J. Polym. Sci., Part C: Polym. Lett.* **1975**, *13*, 39−43.
(37) Schelten, J.; Ballard, D. G. H.; Wignall, G. D.; Longman, G.; Schmatz, W. Small-angle neutron scattering studies of molten and crystalline polyethylene. *Polymer* **1976**, *17*, 751−757.
(38) Mandelkern, L.; Alamo, R. G. In *Polymer Data Handbook*; Mark, J. E., Ed.; Oxford University Press: New York, USA, 1999; pp 493−507.
(39) Fetters, L. J.; Lohse, D. J.; Colby, R. H. In *Physical Properties of Polymer Handbook*, 2nd ed.; Mark, J. E., Ed.; Springer: New York, USA, 1999; pp 447−454.
(40) Abe, A.; Takeda, T.; Hiejima, T. Role of conformation entropy in determining the phase transitions of polymeric systems. *Macromol. Symp.* **2000**, *152*, 255−265.
(41) Mandelkern, L. *Crystallization of Polymers Volume 1 Equilibrium Concepts*, 2nd ed.; Cambridge University Press: New York, USA, 2002; Chapter 6.
(42) Sasanuma, Y.; Watanabe, A. Conformational characteristics of poly(trimethylene sulfide) and structure−property relationships of representative polysulfides and polyethers. *Macromolecules* **2006**, *39*, 1646−1656.
(43) Luinstra, G. A.; Borchardt, E. Material properties of poly(propylene carbonates). *Adv. Polym. Sci.* **2012**, *245*, 29−48.
(44) Takahashi, Y.; Tadokoro, H. Structural studies of polyethers, $(-(CH_2)_m-O-)_n$. X. Crystal structure of poly(ethylene oxide). *Macromolecules* **1973**, *6*, 672−675.
(45) Abe, A.; Furuya, H.; Nam, S. Y.; Okamoto, S. Thermodynamics and molecular ordering of carbonate-type dimer liquid crystals with emphasis on the geometrical characteristics of the linking group. *Acta Polym.* **1995**, *46*, 437−444.
(46) Flory, P. J. *Principles of Polymer Chemistry*; Cornell University Press: Ithaca, NY, USA, 1953.
(47) Flory, P. J.; Hoeve, C. A. J.; Ciferri, A. Influence of bond angle restrictions on polymer elasticity. *J. Polym. Sci.* **1959**, *34*, 337−347.
(48) Flory, P. J.; Ciferri, A.; Hoeve, C. A. J. The thermodynamic analysis of thermoelastic measurements on high elastic materials. *J. Polym. Sci.* **1960**, *45*, 235−236.
(49) Ciferri, A.; Hoeve, C. A. J.; Flory, P. J. Stress-temperature coefficients of polymer networks and the conformational energy of polymer chains. *J. Am. Chem. Soc.* **1961**, *83*, 1015−1022.
(50) Mark, J. E. Thermoelastic results on rubberlike networks and their bearing on the foundations of elasticity theory. *Macromol. Rev.* **1976**, *11*, 135−159.
(51) Mark, J. E. Rubber Elasticity. *J. Chem. Educ.* **1981**, *58*, 898−903.
(52) Flory, P. J. Molecular interpretation of rubber elasticity. Charles Goodyear Medal Address—1968. *Rubber Chem. Technol.* **1968**, *41*, G41−G48.
(53) Abe, A.; Jernigan, R. L.; Flory, P. J. Conformational energies of *n*-alkanes and the random configuration of higher homologs including polymethylene. *J. Am. Chem. Soc.* **1966**, *88*, 631−639.
(54) Thorat, S. D.; Phillips, P. J.; Semenov, V.; Gakh, A. Physical properties of aliphatic polycarbonates made from CO_2 and epoxides. *J. Appl. Polym. Sci.* **2003**, *89*, 1163−1176.
(55) Chen, L.; Qin, Y.; Wang, X.; Zhao, X.; Wang, F. Plasticizing while toughening and reinforcing poly(propylene carbonate) using low molecular weight urethane: Role of hydrogen-bonding interaction. *Polymer* **2011**, *52*, 4873−4880.
(56) Ren, G.; Miao, Y.; Qiao, L.; Qin, Y.; Wang, X.; Wang, F. Toughening of amorphous poly(propylene carbonate) by rubbery CO_2-based polyurethane: Transition from brittle to ductile. *RSC Adv.* **2015**, *5*, 49979−49986.
(57) Li, J.; Lai, M. F.; Liu, J. J. Control and development of crystallinity and morphology in poly(*β*-hydroxybutyrate-*co*-*β*-hydroxyvalerate)/poly(propylene carbonate) blends. *J. Appl. Polym. Sci.* **2005**, *98*, 1427−1436.
(58) Cyriac, A.; Lee, S. H.; Lee, B. Y. Connection of polymer chains using diepoxide in CO_2/propylene oxide copolymerizations. *Polym. Chem.* **2011**, *2*, 950−956.
(59) Abe, A.; Furuya, H.; Mitra, M. K.; Hiejima, T. The polyoxyethylene chain—on the origin of its conformational flexibility. *Comput. Theor. Polym. Sci.* **1998**, *8*, 253−258.
(60) Pedersen, C. J. Cyclic polyethers and their complexes with metal salts. *J. Am. Chem. Soc.* **1967**, *89*, 7017−7036.
(61) Tominaga, Y.; Yamazaki, K. Fast Li-ion conduction in poly(ethylene carbonate)-based electrolytes and composites filled with TiO_2 nanoparticles. *Chem. Commun.* **2014**, *50*, 4448−4450.
(62) Tominaga, Y. Ion-conductive polymer electrolytes based on poly(ethylene carbonate) and its derivatives. *Polym. J.* **2017**, *49*, 291−299.
(63) Zhang, J.; Zang, X.; Wen, H.; Dong, T.; Chai, J.; Li, Y.; Chen, B.; Zhao, J.; Dong, S.; Ma, J.; Yue, L.; Liu, Z.; Guo, X.; Cui, G.; Chen, L. High-voltage and free-standing poly(propylene carbonate)/$Li_{6.75}La_3Zr_{1.75}Ta_{0.25}O_{12}$ composite solid electrolyte for wide temperature range and flexible solid lithium ion battery. *J. Mater. Chem. A* **2017**, *5*, 4940−4948.
(64) Jeromin, G. E. Production of carbonate esters from alcohol and chloroformate, used as perfumes and aroma agents. German Patent DE 19802198A1, 1999.
(65) Budzelaar, P. H. *gNMR*, Version 5.0; IvorySoft & Adept Scientific plc: Letchworth, U.K., 2004.
(66) Sasanuma, Y. Solvent effect on the conformation of 1,2-dimethoxypropane. *J. Phys. Chem.* **1994**, *98*, 13486−13488.
(67) Frisch, M. J.; et al. *Gaussian 09*, Revision B01; Gaussian Inc: Wallingford CT, USA, 2009.
(68) Cancès, E.; Mennucci, B.; Tomasi, J. A new integral equation formalism for the polarizable continuum model: theoretical background and applications to isotropic and anisotropic dielectrics. *J. Chem. Phys.* **1997**, *107*, 3032−3041.
(69) Mattice, W. L.; Suter, U. W. *Conformational Theory of Large Molecules: The Rotational Isomeric State Model in Macromolecular Systems*; Wiley-Interscience: New York, USA, 1994.
(70) Sasanuma, Y.; Touge, D. Configurational statistics of poly(L-lactide) and poly(DL-lactide) chains. *Polymer* **2014**, *55*, 1901−1911.

DOI: 10.1021/acsomega.7b00964
ACS Omega 2017, 2, 4808−4819